Favorable Propagation for Wideband Massive MIMO with Non-Uniform Linear Arrays

Elham Anarakifirooz, Sergey Loyka

***Abstract*—Favorable propagation (FP) for massive MIMO with uniform and non-uniform linear arrays is studied. A gap in the existing FP studies of uniform linear arrays is identified, which is related to the existence of grating lobes in the array pattern and which results in the FP condition being violated, even under distinct angles of arrival. A novel analysis and design of *non-uniform* linear arrays are proposed to cancel grating lobes and to restore favorable propagation for *all* distinct angles of arrival. This design is based on a subarray structure and fits well with efficient hybrid beamforming structures proposed for 5/6G systems. In addition, we show that the proposed design is *robust* in the frequency domain and can be used for wideband or ultra-wideband systems.**

I. Introduction

Massive MIMO is widely accepted as one of the key technologies for 5G and beyond. It provides significant improvements in spectral and energy efficiencies as well as simplified processing in multi-user environments, due to a phenomenon known as "favorable propagation" (FP), whereby the channel vectors of different users become orthogonal to each other as the number of antennas increases [1][2]. While channel vectors of different users are rarely exactly orthogonal to each other in practice, it has been shown theoretically and experimentally that the FP holds approximately in many scenarios of practical interest so that the benefits of massive MIMO can be exploited [1]-[9].

Favorable propagation for uniform linear arrays (ULA) was studied analytically in [1]-[5] and experimentally in [6]-[9]. Antenna array geometry and propagation environment along with users' locations were identified as the key factors determining the existence or non-existence of the FP. It was concluded that, for a fixed antenna element spacing and LOS propagation, the FP holds asymptotically (as the number N of antenna elements increases without bound) as long as users have distinct angles of arrival (AoA). In this Paper, we show that this conclusion is based on an implicit assumption (not mentioned in the above studies) that there are no grating lobes (GL) in the array pattern and that it fails to hold if GLs are present (which is determined by the element spacing and beam steering) and some users align with their directions.

Larger element spacing under fixed N (i.e. fixed complexity/cost) is desirable to increase the array spatial resolution (or, equivalently, to decrease its beamwidth), i.e. its ability to resolve nearby users and hence to cancel inter-user inference (IUI). However, this has a major drawback as grating lobes appear in the array pattern for larger spacing [10][11] so that different users appearing at the main beam and GLs directions cannot be resolved, which creates significant IUI at those directions. This has a profound negative impact on favorable propagation, even under distinct AoAs. The larger the antenna spacing, the more grating lobes will appear and so more directions should be banned for other users to maintain the FP. An experimental observation of the grating lobe's effect on IUI and favorable propagation was reported in [9], but, to the best of our knowledge, no comprehensive *analysis* is available in the literature, so that the existing FP analysis for ULAs is incomplete in this respect. No design to eliminate the impact of GLs on favorable propagation was proposed either.

To address these issues, we present a rigorous analysis of grating lobes' impact on favorable propagation (see Propositions 1 and 2) and propose a non-uniform linear array (NULA) design that effectively cancels grating lobes and thus ensures that the FP holds for any element spacing and any distinct AoAs (see Theorem 1). The NULA design we propose is block-partitioned, whereby each block (subarray) is an ULA but the overall array is not uniform. In order to cancel GLs, we show that the number N_b of subarrays (blocks) and their spacing ΔD have to be carefully selected so that, asymptotically, grating lobes are cancelled by nulls in the block array factor and thus the FP is restored for any distinct AoAs. To this end, we use some concepts from number theory, which, to the best of our knowledge, have not been used before in massive MIMO or antenna array literature. It should be noted that while the actual number of grating lobes and their directions do depend on the main beam direction (i.e. beam steering), see e.g. [10][11], the design we propose is independent of it, so it can accommodate beam steering and grating lobes are canceled for any direction of the main beam. The proposed block-partitioned array structure fits well with efficient designs proposed for 5/6G systems, which make use of subarrays and hybrid beamforming [12][13].

Data rates demands continue their exponential growth due to e.g. popular applications (HD video streaming) as well as the increase in the number of wireless devices. 5G systems make use of wide bandwidth (up to 400 MHz per channel) to address this demand (along with other technologies such as massive MIMO) [17, section 3.1.2]. 6G systems are envisioned to have even larger bandwidth available at millimeter wave and THz bands (e.g. up to 50 GHz as in IEEE 802.15.3d)[18]. While OFDM-type techniques handle efficiently frequency-selective properties of a wideband channel, antenna array design is much more challenging for wide bandwidth [10][11]. In particular, unlike signal processing techniques, antenna array geometry cannot change on a sub-carrier basis. Hence, frequency-independent geometric design is needed. To address this issue, we show in Sec. V that the above analysis and design are remarkably robust in frequency domain so that they can be applied to wide-band systems as well. Specifically, the FP property of ULA is essentially frequency-independent as long as there are no grating lobes at all frequencies and the

E. Anarakifirooz and S. Loyka are with the School of Electrical Engineering and Computer Science, University of Ottawa, Ontario, Canada, e-mail: sergey.loyka@ieee.org

2022 17th Canadian Workshop on Information Theory (CWIT) | 978-1-6654-9908-8/22/$31.00 ©2022 IEEE | DOI: 10.1109/CWIT55308.2022.9817666

block-partitioned NULA design in Theorem 1 also holds over a wideband channel provided the number of blocks is properly selected (based on the largest frequency, see Proposition 3).

II. Channel Model and Favorable Propagation

Let us consider a Gaussian MIMO channel, where M independent single-antenna users transmit simultaneously to a base station (BS) equiped with an N-element antenna array:

$$\boldsymbol{y} = \boldsymbol{h}_1 x_1 + \sum_{i=2}^{M} \boldsymbol{h}_i x_i + \boldsymbol{\xi} \tag{1}$$

where $\boldsymbol{h}_i, x_i$ are the channel (column) vector and the transmitted signal of user i, $i = 1, ..., M$; $\boldsymbol{y}, \boldsymbol{\xi}$ are the received BS signal and noise vectors, respectively; $|\boldsymbol{h}|, \boldsymbol{h}'$ and $\boldsymbol{h}^+$ denote Euclidean norm (length), transposition and Hermitian conjugation, respectively, of vector $\boldsymbol{h}$. The noise is Gaussian circularly symmetric, of zero mean and variance σ_0^2 per Rx antenna. Following [1][3][4], we consider a far-field LOS-dominated environment, as in e.g. mmWave or THz systems where LOS is essential to maintain a proper link SNR [14][18].

To simplify the decoding process, the BS uses linear processing with matched filter beamforming $w = \boldsymbol{h}_1/|\boldsymbol{h}_1|$ to decode user 1, treating other users' signals as interference. Hence, its SINR can be expressed as follows:

$$\text{SINR} = \frac{|\boldsymbol{h}_1|^2 \sigma_{x_1}^2}{|\boldsymbol{h}_1|^{-2} \sum_{i=2}^{M} |\boldsymbol{h}_1^+ \boldsymbol{h}_i|^2 \sigma_{x_i}^2 + \sigma_0^2} \tag{2}$$

$$= \gamma_1 \left(\sum_{i=2}^{M} |\alpha_{iN}|^2 \gamma_i + 1 \right)^{-1}, \quad \alpha_{iN} = \frac{\boldsymbol{h}_1^+ \boldsymbol{h}_i}{N} \tag{3}$$

where σ_{xi}^2 and $\gamma_i = |\boldsymbol{h}_i|^2 \sigma_{xi}^2 / \sigma_0^2$ are the signal power and the SNR of user i; the channel is normalized so that $|\boldsymbol{h}_i|^2 = N$ (this is consistent with the far-field LOS model in (8)) while the propagation path loss is absorbed into the respective Rx SNR γ_i. Using this simplified decoding method, the SINR cannot exceed the single-user SNR γ_1,

$$\text{SINR} \le \gamma_1 \tag{4}$$

and this maximum is attained when the users' channels become orthogonal to each other,

$$\text{SINR} \to \gamma_1 \ \text{ if } \ \alpha_{iN} \to 0 \ \forall \ i > 1 \tag{5}$$

as the number N of antenna elements increases and all SNRs stay uniformly bounded, i.e. $\gamma_i \le \gamma_{max} < \infty$ for some γ_{max} independent of N (where γ_i may depend on N). This is known as (asymptotically) favorable propagation (FP) condition. When the number of users is finite, the FP condition can be expressed in 2 equivalent ways:

$$\lim_{N\to\infty} \alpha_N^2 = 0 \quad \Leftrightarrow \quad \lim_{N\to\infty} |\alpha_{iN}| = 0 \ \forall i > 1 \tag{6}$$

where $\alpha_N^2 = \sum_{i=2}^{M} |\alpha_{iN}|^2$ characterizes the total interference leakage and $|\alpha_{iN}|^2$ represents IUI power "leakage" from user i to the main user. If all users have the same SNR ($\gamma_i = \gamma_1$), then the SINR simplifies to:

$$\text{SINR} = (\alpha_N^2 + \gamma_1^{-1})^{-1} \le \gamma_1 \tag{7}$$

and, under favorable propagation, the upper bound is attained, SINR $= \gamma_1$. While in practice the number N of elements is always finite and α_N^2 is never exactly zero, the FP is closely approached if $\alpha_N^2 \ll \gamma_1^{-1}$ so that SINR $\approx \gamma_1$. This justifies the asymptotic analysis $N \to \infty$ from the practical perspective, since, if the asymptotic FP (6) holds, it follows from the limit definition that there exists a sufficiently large N for which $\alpha_N^2 \ll \gamma_1^{-1}$ and thus SINR $\approx \gamma_1$. This is no longer the case if the FP does not hold.

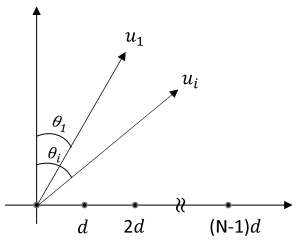

Fig. 1. An illustration of ULA(N, d), where u_i is a unitary vector directed to user i and θ_i is its AoA while the main user is at θ_1, all measured from broadside; $-\pi/2 \le \theta_1,\ \theta_i \le \pi/2$. When 1st user's signal is decoded, i-th user is a source of interference.

III. Favorable propagation for ULAs

Favorable propagation for uniform linear arrays has been investigated analytically and experimentally [1]-[9]. It was concluded that FP holds asymptotically for ULAs of fixed element spacing under LOS propagation conditions and distinct users' AoAs [1][3][4] but does not hold if the antenna array size is fixed (so that the element spacing decreases when N increases) [5]. However, the former conclusion is based on the implicit assumption, not stated in the above studies, that there are no grating lobes in the array factor and it does not hold if GLs are present. To see this, observe that [1, eq. (7.17)], which is equivalent to eq. (9) below with minor notational differences, converges to 0 as $N \to \infty$ only if its denominator is not zero. However, the denominator is indeed zero if GLs are present in the antenna array pattern, even under distinct users' AoAs, as the example below shows. This observation also applies to [4, eq. (18)] and [3, eq. (34), (42)]. In particular, Propositions 4 and 5 in [3] fail to hold if GLs are present.

Example 1: consider a ULA of isotropic elements with element spacing $d = 1/2$ measured in wavelengths, as illustrated in Fig. 1. Let $\theta_1 = 90^o$ and $\theta_i = -90^o \ne \theta_1$ (i.e., distinct AoAs). It is straightforward to see that, in this case, the denominator in [1, eq. (7.17)] is zero and the respective scalar product $|\alpha_{iN}| = 1$ for any N, see (9) below, i.e. the FP fails to hold even though the AoAs are distinct. The same observation applies to [4, eq. (18)] and [3, eq. (34), (42)]. This can be explained via the array factor shown in Fig. 4, where the main beam is at $\theta_1 = 90^o$ to follow user 1 while the grating lobe appears at -90^o, so that, if another user is at the latter direction, it cannot be discriminated from the 1st user and hence the FP fails to hold (even though the AoAs here are distinct). Even if the main user is at broadside, i.e. $\theta_1 = 0^o$, grating lobes appear if $d \ge 1$ and the FP fails to hold, even under distinct AoAs, e.g. if $d = 1,\ \theta_1 = 0^o,\ \theta_i = \pm\pi/2$, see Fig. 3, which also results in zero denominators in [3][4]. In general, the larger d, the more grating lobes emerge [10][11] and favorable propagation fails to hold if users' AoAs, being distinct from each other, coincide with the GL directions. Eq. (12) below gives precise condition for this to happen.

978-1-6654-9908-8/22/$31.00 ©2022 IEEE

To analyze the impact of grating lobes on favorable propagation, we follow [1][3][4] and consider LOS-dominated environment, where users have distinct angles-of-arrival (AoAs). In the far-field, the normalized channel vector of i-th user for N-element ULA of isotropic elements with element spacing d (measured in wavelengths) is:

$$\boldsymbol{h}_i = [e^{j\psi_{0i}}, \cdots, e^{j\psi_{(N-1)i}}]', \quad i = 1, \cdots, M \qquad (8)$$
$$\psi_{ni} = 2\pi n d \sin(\theta_i), \quad n = 0, \cdots, N-1$$

where θ_i is the AoA of user i signal of which there are M, $-\pi/2 \le \theta_i \le \pi/2$; ψ_{ni} is the phase shift at element n with respect to 1st element, see Fig. 1. All users are assumed to be in the front half-plane, $-\pi/2 \le \theta_i \le \pi/2$, and there is no backward radiation (usually eliminated by a ground plane or by array elements). For further reference, we use $\mathrm{ULA}(N, d)$ to denote a uniform linear array with N isotropic elements and element spacing d. Using the system model in (1), the inter-user interference leakage from user i to the main user ($i = 1$) can be expressed as follows:

$$\alpha_{iN} = N^{-1}\boldsymbol{h}_1^+\boldsymbol{h}_i = \frac{\sin(N\Delta\psi_i/2)}{N\sin(\Delta\psi_i/2)} e^{j(N-1)\Delta\psi_i/2} \qquad (9)$$

where $\Delta\psi_i = 2\pi d(\sin\theta_i - \sin\theta_1)$. Further notice that $\lim_{N\to\infty}\alpha_{iN} = 0$, i.e. the FP holds, provided that $\sin(\Delta\psi_i/2) \neq 0$. The latter condition may be violated even if $\theta_i \neq \theta_1$ (distinct AoAs), e.g. if $d = 1,\ \theta_1 = 0,\ \theta_i = \pm 90^o \neq \theta_1$ so that $\Delta\psi_i = \pm 2\pi$, $\sin(\Delta\psi_i/2) = 0$ and hence $|\alpha_{iN}| = 1$ for any N. This represents a grating lobe in the array pattern, see e.g. [10][11]. In general, GL directions ϕ_k correspond to zero denominator in (9), i.e. $\sin(\Delta\psi_i/2) = 0$, and, for a given θ_1, can be found from $\Delta\psi_i = 2\pi k$ with $\theta_i = \phi_k$, which is equivalent to

$$\sin(\phi_k) = \sin(\theta_1) + k/d \qquad (10)$$

where k is the GL index, $k = \pm 1, \pm 2, ...$ Since $|\sin\phi_i| \le 1$, there exist no grating lobes if

$$d(1 + |\sin\theta_1|) < 1 \qquad (11)$$

In this case, the results in [1][3][4] do hold for any distinct θ_i, but they may fail to hold if (11) is not satisfied. Indeed, using (9), it follows that, under distinct AoAs $\theta_i \neq \theta_1$,

$$\lim_{N\to\infty}|\alpha_{iN}| = \begin{cases} 1, \text{if } d(1+|\sin\theta_1|) \ge 1 \ \&\ \theta_i = \phi_k \\ 0, \text{ otherwise.} \end{cases} \qquad (12)$$

Note a dichotomy here: the limit is either zero or one. The latter case gives the conditions when the FP fails to hold: $d(1+|\sin\theta_1|) \ge 1$ is the condition for the GL existence, and $\theta_i = \phi_k$ is the condition for i-th user AoA to coincide with k-th GL direction. These are precisely the cases overlooked in [1][3][4]. Note from (12) that the FP may fail to hold even if $d = 1/2$ (as in [1, eq. (7.17)]), e.g. if $\theta_1 = 90^o$, $\theta_i = \phi_{-1} = -90^o \neq \theta_1$ so that $\Delta\psi_i = -2\pi$, $\sin(\Delta\psi_i/2) = 0$ and $|\alpha_{iN}| = 1$ for any N, but the FP always holds if $d < 1/2$.

To determine the number of grating lobes, observe that $|\sin(\phi_k)| \le 1$ and use (10) to obtain the range of k:

$$k \ge k_{min} = -\lfloor d(1+\sin(\theta_1))\rfloor \ge -\lfloor 2d\rfloor \qquad (13)$$
$$k \le k_{max} = \lfloor d(1-\sin(\theta_1))\rfloor \le \lfloor 2d\rfloor \qquad (14)$$

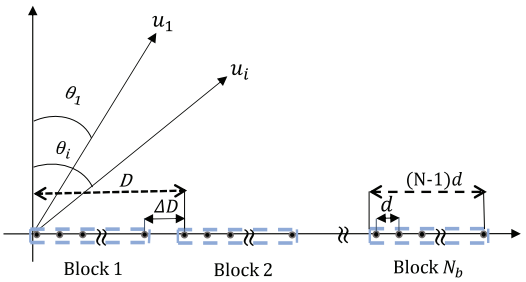

Fig. 2. Block-partitioned NULA of N_b subarrays (blocks) $\mathrm{ULA}(N, d)$ with subarray spacing ΔD; $D = (N-1)d + \Delta D$, and $(N-1)D$ is the subarray length. The AoAs are distinct, $\theta_1 \neq \theta_i$, and $-\pi/2 \le \theta_1,\ \theta_i \le \pi/2$.

where $\lfloor\cdot\rfloor$ is the floor function, so that $I_k = \{\{k_{min}, \cdots, k_{max}\} - \{0\}\}$ is the GL index set, $k = 0$ represents the main beam and hence is excluded; I_k is an empty set if there are no GLs. Thus, the number K of GLs does not exceed $\lfloor 2d\rfloor$,

$$K = k_{max} - k_{min} \le \lfloor 2d\rfloor \qquad (15)$$

and there are no grating lobes if $d < 1/2$, for any θ_1.

Motivated by the above analysis of grating lobes and their impact on the FP, we present below a structural design of nonuniform linear arrays that eliminates grating lobes and guarantees FP to hold for any distinct AoAs.

IV. Non-uniform Linear Array Design for FP

This section aims to exploit a non-uniform array structure to cancel grating lobes and hence to achieve favorable propagation for all distinct AoAs and any element spacing d. We consider a block-partitioned non-uniform array as in Fig. 2: the overall NULA consists of N_b subarrays (blocks), which are $\mathrm{ULA}(N, d)$ and which are arranged in the $\mathrm{ULA}(N_b, D)$ block-wise pattern. The overall NULA pattern is a product of the subarray factor of $\mathrm{ULA}(N, d)$ and the block array factor of $\mathrm{ULA}(N_b, D)$ (where each block is replaced with an isotropic element), see e.g. [10, p. 75][11, p. 7]. Thus, the GLs in the subarray factor can be cancelled with nulls in the block array factor, as explained below. Finding proper N_b and the subarray spacing ΔD are crucial to cancel all GLs and hence to achieve favorable propagation for any distinct AoAs and any d.

Due to the block-wise symmetry of the structure, the overall channel vector $\boldsymbol{h}_i$ of the NULA for user i can be expressed as follow:

$$\boldsymbol{h}_i = \boldsymbol{h}_{si} \otimes \boldsymbol{h}_{bi} \qquad (16)$$

where $\otimes$ denotes Kronecker product; $\boldsymbol{h}_{si}$ and $\boldsymbol{h}_{bi}$ represents the channel vector of the subarray $\mathrm{ULA}(N, d)$ and of the block array $\mathrm{ULA}(N_b, D)$, respectively, where $\boldsymbol{h}_{si}$ is as in (8) and $\boldsymbol{h}_{bi}$ is

$$\boldsymbol{h}_{bi} = [e^{j\psi_{b,0i}}, \cdots, e^{j\psi_{b,(N_b-1)i}}]', \quad i = 1, \cdots, M \qquad (17)$$
$$\psi_{b,ni} = 2\pi n D \sin(\theta_i), \quad n = 0, \cdots, N_b - 1$$

For further use, the interference leakage terms of the NULA are defined as follows:

$$\alpha_{iN} = \frac{\boldsymbol{h}_1^+\boldsymbol{h}_i}{N_b N},\ \alpha_{siN} = \frac{\boldsymbol{h}_{s1}^+\boldsymbol{h}_{si}}{N},\ \alpha_{bi} = \frac{\boldsymbol{h}_{b1}^+\boldsymbol{h}_{bi}}{N_b} \qquad (18)$$

978-1-6654-9908-8/22/$31.00 ©2022 IEEE

where α_{siN} and α_{bi} represent the respective terms for a single subarray $\mathrm{ULA}(N,d)$ and the block array $\mathrm{ULA}(N_b,D)$ while α_{iN} represents the overall leakage.

The following proposition is instrumental in establishing the FP for the block-partitioned NULA.

Proposition 1. *Let $\boldsymbol{h}_i$ have Kronecker structure as in* (16)*. Then, α_{iN} can be expressed and bounded as follows:*

$$\alpha_{iN} = \alpha_{siN}\alpha_{bi} \tag{19}$$
$$|\alpha_{iN}| \le \min\{|\alpha_{siN}|, |\alpha_{bi}|\} \tag{20}$$

Proof. Observe the following:

$$\begin{aligned}\alpha_{iN} &= (N_bN)^{-1}\boldsymbol{h}_1^+\boldsymbol{h}_i \\ &= (N_bN)^{-1}(\boldsymbol{h}_{s1}\otimes\boldsymbol{h}_{b1})^+(\boldsymbol{h}_{si}\otimes\boldsymbol{h}_{bi}) \\ &= (N_bN)^{-1}(\boldsymbol{h}_{s1}^+\otimes\boldsymbol{h}_{b1}^+)(\boldsymbol{h}_{si}\otimes\boldsymbol{h}_{bi}) \\ &= (N^{-1}\boldsymbol{h}_{s1}^+\boldsymbol{h}_{si})(N_b^{-1}\boldsymbol{h}_{b1}^+\boldsymbol{h}_{bi}) = \alpha_{siN}\alpha_{bi}\end{aligned} \tag{21}$$

where 3rd and 4th equalities are due to the properties of Kronecker products [15]. The inequality in (20) follows from $|\alpha_{siN}|,\ |\alpha_{bi}| \le 1$. □

Thus, the impact of subarray and block array factors α_{siN}, α_{bi} on the overall IUI leakage factor α_{iN} is factorized, which simplifies the analysis considerably. In particular, using (20), $|\alpha_{iN}| \to 0$ if either $|\alpha_{siN}| \to 0$ or $|\alpha_{bi}| \to 0$. This can be exploited to cancel grating lobe's effect on the FP. To this end, let us consider the asymptotic ("massive") regime where $N \to \infty$ while N_b is fixed (constant), under distinct AoAs.

Proposition 2. *If N_b is fixed and $\theta_1 \neq \theta_i$, then the following asymptotic relationship holds for the block-portioned NULA:*

$$\lim_{N\to\infty} |\alpha_{iN}| = \begin{cases} |\alpha_{bi}(\phi_k)|, & \exists k \in I_k:\ \theta_i = \phi_k \\ 0, & \text{otherwise}. \end{cases} \tag{22}$$

Proof. Using (20),

$$\lim_{N\to\infty} |\alpha_{iN}| = 0 \text{ if } \theta_i \neq \theta_1 \ \&\ \theta_i \neq \phi_k\ \forall k \in I_k \tag{23}$$

since, from (12), $\lim_{N\to\infty}|\alpha_{siN}| = 0$ in this case. On the other hand, if $\theta_i = \phi_k$ for some $k \in I_k$, then $|\alpha_{iN}| = |\alpha_{bi}(\phi_k)|$ since $|\alpha_{siN}| = 1$ in this case. Note from (18) that, in this case,

$$\begin{aligned}\alpha_{bi}(\phi_k) &= \frac{1}{N_b}\sum_{n=0}^{N_b-1} e^{j2\pi nD(\sin(\phi_k)-\sin(\theta_1))} \\ &= \frac{1}{N_b}\frac{\sin(\pi N_b k\Delta D/d)}{\sin(\pi k\Delta D/d)}e^{j\pi N_b k\Delta D/d}\end{aligned} \tag{24}$$

where the last equality is from (10) and $D = (N-1)d + \Delta D$. Thus, $\alpha_{bi}(\phi_k)$ is independent of N and this proves the 1st case in (22). □

From (22), the FP is guaranteed under distinct AoAs if users do not align with grating lobes (or if GLs do not exist), $\theta_i \neq \phi_k\ \forall\ k \in I_k$. If some users do align, then the following equivalence holds:

$$\lim_{N\to\infty} \alpha_{iN} = 0 \quad \Leftrightarrow \quad \alpha_{bi}(\phi_k) = 0\ \forall k \in I_k \tag{25}$$

i.e. grating lobes are canceled and the FP holds under *any* distinct AoAs if $\alpha_{bi}(\phi_k) = 0\ \forall k \in I_k$. The latter can be achieved by exploiting the NULA structure and choosing appropriate values of N_b and ΔD as shown below.

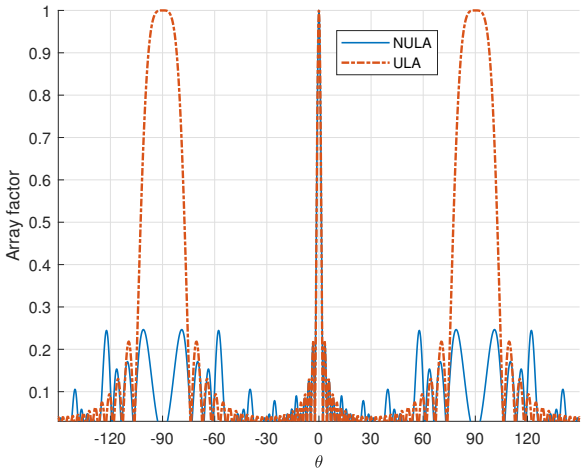

Fig. 3. Array factor of a ULA with $N = 25$ and $d = 1$. While the main beam is at $\theta_1 = 0^o$, note the presence of grating lobes at $\theta_2 = \pm 90^o$. The proposed NULA design with $N = 5,\ N_b = 5, p = 4$ partially cancels these grating lobes.

To this end, we need the following concepts from number theory [16, p. 231]:

- *Greatest common divisor* of two integer m and n, $\gcd(m,n)$: the largest positive integer that devides m and n without remainder; e.g. $\gcd(15,12) = 3$.
- *Coprime (relative prime)*: two numbers n and m are coprime if $\gcd(n,m) = 1$ (no common divisors); e.g. $\gcd(3,5) = 1$, so, 3 and 5 are coprime. If $\gcd(n,m) = 1$ and $n, m > 1$, then n/m or m/n are not integer.

The following theorem presents the NULA design to cancel grating lobes and to achieve favorable propagation under any distinct AoAs.

Theorem 1. *In LOS environment, favorable propagation holds asymptotically ($N \to \infty$) for the NULA comprised of N_b subarrays $\mathrm{ULA}(N,d)$, as in Fig. 2, with subarray spacing $\Delta D > 0$, any fixed element spacing $d > 0$ and any distinct users' AoAs, $\theta_1 \neq \theta_i$, if:*

$$\text{(a)}\ \ N_b > \lfloor 2d \rfloor \ \text{ and (b)}\ \ \Delta D = pd/N_b, \tag{26}$$

where p is a positive integer coprime with N_b, i.e. $\gcd(p, N_b) = 1$, and there is no backward radiation.

Proof. The proof is based on the following 3 key steps. (i) Use (22) and ensure that $\alpha_{bi}(\phi_k) = 0\ \forall k \in I_k$. To achieve this, (ii) select ΔD as in (26)(b) so that each GL is cancelled by a null in the block-array factor. (iii) Select N_b as in (26)(a) to make sure there are enough nulls to cancel all grating lobes. The details are omitted due to the page limit. □

An example of NULA design using Theorem 1, is illustrated in Fig. 3, where the grating lobes of a ULA with $d = 1, \theta_1 = 0^o$ occur at $\pm 90^o$. Designing a non-uniform structure using $N_b = 5 > \lfloor 2d \rfloor$ and $p = 4$ (coprime with N_b) which results in $\Delta D = pd/N_b = 4/5$, partially cancells the grating lobes.

V. Extension to Wideband Channels

While the above analysis and design apply to a single carrier frequency, as typical for antenna arrays, it remains to be seen whether they still hold for wide or ultra-wideband

978-1-6654-9908-8/22/$31.00 ©2022 IEEE

systems, as typical for 5/6G systems, which use multiple subcarriers, as in wideband OFDM or with bandwdith agregation. In this section, we demonstrate that the proposed NULA design demonstrates a remarkable robustness property in the frequency domain and therefore is applicable to wideband or ultra-wideband channels.

To this end, let us consider an LOS channel with operating frequency range $[f_1, f_2]$, which corresponds to the wavelength interval $[\lambda_2, \lambda_1]$, and let d and ΔD be physical distances, measured in meters (not in wavelengths); $\mathrm{ULA}(N, d)$ will represent an N-element ULA of the physical element spacing d. We impose *no limitation* on bandwidth. The following Proposition extends Theorem 1 to a wideband setting.

Proposition 3. *Consider an LOS channel operating over a (wide) frequency range $[f_1, f_2]$ under the conditions of Theorem 1. Then, favorable propagation holds asymptotically over the entire frequency range for a NULA comprised of N_b subarrays $\mathrm{ULA}(N, d)$ with subarray spacing ΔD if:*

$$\text{(a)}\ \ N_b > \lfloor 2d/\lambda_2 \rfloor \ \text{ and (b)}\ \ \Delta D/d = p/N_b, \qquad (27)$$

where d is the physical element spacing and p is a positive integer coprime with N_b.

Proof. Let $K(\lambda)$ be the number of grating lobes at wavelength $\lambda \in [\lambda_2, \lambda_1]$. Using (15),

$$K(\lambda) \le \lfloor 2d/\lambda \rfloor \le \lfloor 2d/\lambda_2 \rfloor, \quad \forall \lambda \ge \lambda_2 \qquad (28)$$

In particular, there are no grating lobes for any $\lambda \ge \lambda_2$ if $d < \lambda_2/2$, which is remarkable robustness property as it also applies to wide and ultra-wideband channels. Now, (27)(a) ensures that there are enough nulls in the block array factor to cancel all grating lobes. Condition (27)(b) ensures that those nulls do align with GL directions. It follows directly from (26)(b) since the latter is frequency-independent (both sides can be multiplied by λ to obtain physical distances). □

Comparing (27) to (26), note that a wideband or ultra-wideband setting requires N_b to be set based on the highest frequency or shortest wavelength; there is no any specific limitation related to bandwidth here.

To illustrate Proposition 3 for a finite number of elements, we apply it to *Example 1* above with $d = \lambda_2/2, \theta_1 = 90^\circ$ (this corresponds to an endfire array, which are often used in practice, see e.g. [10, Sec. 2.5][11, Sec. 9.2][13][19, Sec. 6.3.2]), and set $f_1 = 0.8 f_2$. It follows from (27) that $N_b > \lfloor 2d/\lambda_2 \rfloor = 1$ so that setting $N_b = 5, p = 4$ (coprime with N_b), $\Delta D = pd/N_b = 2\lambda_2/5$ satisfies the conditions of Proposition 3. Fig. 4 shows that this design partially cancels the GL even with finite $NN_b = 25$. It should be pointed out that this selection of $N_b, p, \Delta D$ guarantees GL cancellation for any main beam direction θ_1 (not only $\theta_1 = 90^o$) and any $f \le f_2$, i.e. for a wideband or ultra-wideband channel.

Fig. 4 suggests that even the single carrier frequency design at f_1 can be significantly improved (better GL cancellation) by designing at a slightly higher frequency f_2 instead, which corresponds to using a smaller d.

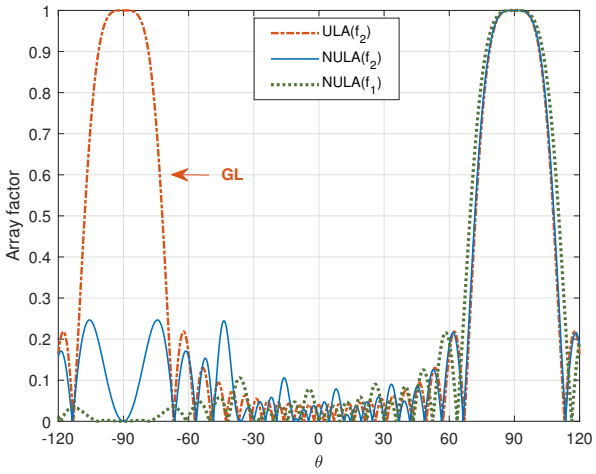

Fig. 4. Array factors of $\mathrm{ULA}(25, d)$ and the NULAs at corresponding frequencies, with $f_1 = 0.8 f_2$, and $d = \lambda_2/2$. While the main beam is at $\theta_1 = 90^o$, note the presence of a grating lobe in the ULA factor at $\theta_2 = -90^o$. The proposed NULA design with $N = 5$, $N_b = 5, p = 4$ partially cancels this grating lobe over the entire frequency range, with better cancellation at f_1.

VI. Acknowledgement

Insightful discussions with C. D'Amours and H. Yanikomeroglu are greatly acknowledged.

References

[1] T. L. Marzetta et al., Fundamentals of Massive MIMO, Cambridge Univ. Press, 2016.
[2] H. Q. Ngo, E. G. Larsson, and T. L. Marzetta, Energy and Spectral Efficiency of Very Large Multiuser MIMO Systems, IEEE Trans. Comm., vol. 61, no. 4, pp. 1436–1449, Apr. 2013.
[3] J. H. Chen, When Does Asymptotic Orthogonality Exist for Very Large Arrays ? IEEE GlobeCom, Atlanta, GA, USA, pp. 4146-4150, Nov. 2013.
[4] H.Q. Ngo, E.G. Larsson, T.L Marzetta, Aspects of Favorable Propagation in Massive MIMO, 22nd European Sig. Proc. Conf. (EUSIPCO), Lisbon, Portugal, pp. 76–80, Sep. 2014.
[5] C. Masouros, M. Matthaiou, Physically Constrained Massive MIMO: Hitting the Wall of Favorable Propagation, IEEE Comm. Lett., vol. 19, no. 5, pp. 771-–774, May 2015.
[6] J. Hoydis, C. Hoek, T. Wild, S. ten Brink, Channel Measurements for Large Antenna Arrays, in Proc. Int. Symp. Wireless Comm. Syst. (ISWCS), Paris, France, pp. 811-–815, Aug. 2012.
[7] M. Gauger et al, Channel Measurements with Different Antenna Array Geometries for Massive MIMO Systems, 10th Int. ITG Conf. Systems Comm. Coding (SCC), Hamburg, Germany, Feb. 2015.
[8] X. Gao, O. Edfors, F. Rusek, and F. Tufvesson, Massive MIMO Performance Evaluation Based on Measured Propagation Data, IEEE Trans. Wireless Comm., vol. 14, no. 7, pp. 3899-–3911, Jul. 2015.
[9] A. O. Martinez, J. Ø. Nielsen, E. De Carvalho, and P. Popovski, An experimental study of massive MIMO properties in 5G scenarios, IEEE Trans. Antennas Propag., vol. 66, no. 12, pp. 7206—7215, Dec. 2018.
[10] H.L. Van Trees, Optimum Array Processing, Wiley, 2002.
[11] R.C. Hansen, Phased Array Antennas, New York, USA: Wiley, 1998.
[12] A. Puglielli et al., Design of energy-and cost-efficient massive MIMO arrays, Proc. IEEE, vol. 104, no. 3, pp. 586–606, Mar. 2016.
[13] C.N. Chen et al, 38-GHz Phased Array Transmitter and Receiver Based on Scalable Phased Array Modules With Endfire Antenna Arrays for 5G MMW Data Links, IEEE Trans. Microwave Theory Tech., vol. 69, no. 1, pp. 980–999, Jan. 2021.
[14] E.G. Larsson, T.L. Marzetta, H.Q. Ngo, and H. Yang, Antenna Count for Massive MIMO: 1.9 GHz vs. 60 GHz, IEEE Comm. Mag., vol. 56, no. 9, pp. 132–137, Sep. 2018.
[15] J.R. Magnus, H. Neudecker, Matrix Differential Calculus with Applications to Statistics and Econometrics, Wiley, 1999.
[16] K.H. Rosen (Ed.), Handbook of Discrete and Combinatorial Mathematics, Boca Raton, FL, USA: CRC Press, 1999.
[17] E. Dahlman, S. Parkvall, and J. Skold, 5G NR: The Next Generation Wireless Access Technology. New York, NY, USA: Academic, 2018.
[18] M. Polese et al, Toward End-to-End, Full-Stack 6G Terahertz Networks, IEEE Commun. Mag., vol. 58, no. 11, pp. 48–54, Nov. 2020.
[19] C. A. Balanis, Antenna Theory: Analysis and Design, 4th Ed., John Wiley & Sons, Hoboken, USA, 2016.